

## Research Article

# The Amphoteric Ion Exchange Membrane Based on CS/CMC for Tobacco-Protein Adsorption and Separation from Tobacco Extract

Jun Ling <sup>1</sup>, Yixiao Li <sup>2</sup>, Bo Zhou <sup>1</sup>, Baokun Zhu <sup>1</sup>, Xinru Zhang <sup>3,4</sup>,  
Yonghong Wang <sup>3,4</sup>, Tiandong Zhang <sup>1</sup> and Wanying Feng <sup>3</sup>

<sup>1</sup>Technology Centre, China Tobacco Yunnan Industrial Co. Ltd., Kunming 650231, China

<sup>2</sup>Department of Chemical Engineering, Kansas State University, Manhattan, Kansas 66506, USA

<sup>3</sup>College of Chemistry and Chemical Engineering, Taiyuan University of Technology, Taiyuan, 030024 Shanxi, China

<sup>4</sup>Shanxi Key Laboratory of Gas Energy Efficient and Clean Utilization, Taiyuan, 030024 Shanxi, China

Correspondence should be addressed to Yonghong Wang; wangyonghong666@163.com  
and Tiandong Zhang; 15887129085@139.com

Received 12 October 2018; Accepted 12 February 2019; Published 28 May 2019

Academic Editor: Qinglin Wu

Copyright © 2019 Jun Ling et al. This is an open access article distributed under the Creative Commons Attribution License, which permits unrestricted use, distribution, and reproduction in any medium, provided the original work is properly cited.

A macroporous amphoteric ion exchange membrane was prepared by blending chitosan (CS) and carboxymethylcellulose (CMC) in aqueous solution, with glutaraldehyde as a crosslinking agent and silica particles as porogens. The good compatibility between CS and CMC was confirmed by attenuated total reflectance Fourier-transform infrared spectroscopy (FTIR-ATR). A scanning electron microscope was used to observe the morphology of CS/CMC blend membranes, in which a three-dimensional opening structure was formed, and no phase separation was discovered. Tobacco extract was used as a separation model to get tobacco protein. And the effects of the pH value, adsorption time, CS/CMC content, initial protein concentration, and CS/CMC composition on tobacco protein adsorption were investigated by coomassie blue staining during the adsorption process. The results showed that the maximum adsorption capacity of 271.78 mg/g can be achieved under the condition of pH 6.15, adsorption time of 8 h, initial protein concentration of 1.52 mg/mL, and CS/CMC weight of 0.05 g with a mass ratio of 80:20. Tobacco proteins were successfully separated from tobacco extract by adjusting the pH of the feed and the desorption solutions to change their electrostatic force. It was found that the high desorption capacity and protein desorption efficiency can be achieved at pH 9.40. The blend membranes also demonstrated good reusability after 3 adsorption-desorption cycles.

## 1. Introduction

As one of the important tobacco flavors, tobacco extract has been widely applied to the cigarette industry, which plays an important role in the improvement of cigarette quality [1–3]. Extracted from tobacco or its fragment, tobacco extract usually contains a large quantity of macromolecular substances such as protein, pectin, and starch, which are suspected to have an adverse effect on the quality of tobacco extract [4]. These macromolecular substances are the precursors of harmful substances released by cigarette burning, which can increase irritative smell and produce mixed gases with an adverse effect [5, 6]. Therefore, the removal of macromolecular substances from tobacco extract is of great significance for improving the quality of cigarette and reducing harmful

component release. On the other hand, with deepening research of tobacco protein, it is gradually recognized that tobacco protein, which is an abundant resource, is of high nutritional and commercial values in the food industry [7, 8]. Many researchers attempted to extract and separate tobacco protein from tobacco using aqueous two-phase extraction [9], molecular distillation [10], and supercritical fluid chromatography [11]. However, the outcome remained limited because of the high cost and small production capacity. In these technologies, membrane separation plays an important role in the achievement of high-performance separation especially ion exchange membranes, which takes the advantage of electrostatic interactions between the surface charges of protein and the charged groups on the membranes [12–14].

Ion exchange membranes occupy a relatively large market segment in applications for biomacromolecule separation or concentration. In previous works, many classes of ion exchange membranes have been developed for protein separation. But many of them possess only anion- or cation-exchanged performance [15-17]. Amphoteric ion-exchange membranes contain both weak acidic (negative charge) and basic (positive charge) groups that are randomly attached to the polymer chains. And the net charge of the membrane can be controlled by the pH value of the solution, resulting in some characteristic properties that cannot be exhibited by a single-charged ion-exchange membrane [15, 18]. To obtain the amphoteric ion-exchange membranes, a simple way is to blend the only polycation electrolyte (e.g., chitosan) with the polyanion electrolyte to prepare corresponding amphoteric membranes [19]. CS possesses common characteristics of polycation electrolyte due to positively charged amine groups in acidic condition, which can selectively adsorb negatively charged protein by electrostatic interaction. CMC with characteristics of polyanion electrolyte can selectively adsorb positively charged protein. More importantly, they have good thermodynamic compatibility and miscibility as a result of the similarity in the molecular chain structure. Chen et al. [20] successfully prepared chitosan (CS)/carboxymethylcellulose (CMC) blend membranes. And the protein adsorption performance by these membranes from lysozyme aqueous solutions at different pH values was investigated. The results showed that the maximum adsorption capacity of the macroporous CS/CMC blend membranes was as high as 240 mg/g, while more than 95 wt% of the adsorbed lysozyme was desorbed in a pH 11.8 buffer. The blend membranes also demonstrated good reusability after several adsorption-desorption cycles. They [21] also selected ovalbumin (pI = 4.6) and lysozyme (pI = 11) as model proteins. The adsorption of these two proteins on different CS/CMC blend membranes with different initial protein concentrations at different pH values was investigated in their solution. The results indicated that the maximum adsorption for lysozyme and ovalbumin was at pH 9.2 and 4.8, respectively. And the adsorption capacity of these proteins both increased with the increase of initial protein concentration. However, little attention has been drawn on the tobacco protein adsorption from tobacco extract using amphoteric ion exchange membranes based on CS/CMC.

In this study, CS/CMC blend membranes were prepared by a simple solution-blending method with glutaraldehyde as a crosslinking agent for CS and with silica particles as porogens. The effects of the pH value, CS/CMC content, adsorption time, initial protein concentration, and CS/CMC composition on the protein adsorption properties of CS/CMC blend membranes was investigated in tobacco extract solution. Desorption efficiency of tobacco protein was found to be more than 81.36 wt%, implying that CS/CMC blend membranes could separate proteins from tobacco extract by adsorption-desorption process. Finally, tobacco protein was successfully separated from tobacco extract solution by only changing the pH of the feed and the desorption solution. And the blend membranes have excellent stability.

## 2. Experimental

**2.1. Materials.** Chitosan (CS) (powder, deacetylation degree  $\geq 90\%$ ), carboxymethylcellulose (CMC) (viscosity 300-800 mPa·s), epoxy chloropropane, glutaraldehyde (aqueous solution of 50 wt%), borax, boric acid, acetic acid, phosphoric acid, hydrochloric acid, sodium hydroxide, citric acid, sodium citrate, and disodium hydrogen phosphate were obtained from Jingchun Biochemical Technology Co. Ltd. (Shanghai, China). Tobacco leaves were acquired from the Hongyuhonghe Group. Tobacco extract was obtained following reported protocol [22]. Chromatography silica gel (200-300 mesh) was supplied by Qingdao Haiyang Chemical Co. Ltd. Coomassie Brilliant Blue G-250, and bovine serum albumin was purchased from Alfa Aesar.

**2.2. Preparation of Amphoteric CS/CMC Ion Exchange Membranes.** CS/CMC amphoteric blend membranes were prepared by the following steps. Firstly, chitosan (4 g, deacetylation degree  $\geq 95\%$ ) was dissolved in acetic acid solution (196 g, 2 wt%) to prepare polymer solution with a chitosan concentration of 2 wt%. Undissolved particulates are then removed for further use. Carboxymethylcellulose solution (2 wt%) was prepared by dissolving CMC (2 g) in deionized water (98 g) directly. Secondly, a certain mass ratio of CS to CMC in solution (2 wt%) was added to a round-bottomed flask. Concentrated hydrochloric acid was used to adjust the pH value to 3.0. The solution is mechanically stirred for 30 min. After the agitation, a colorless homogeneous solution was obtained. Thirdly, 23.6 mL (1 g/L) glutaraldehyde solution was added into the flask, while the reaction was carried out in a water bath (60°C) under vigorous stirring for 30 min. Porogen silica gel which was 9 wt% of CS, and CMC was added into the flask under vigorous stirring for 3 h. To obtain a homogeneous porous structure, the porogen silica gel should be distributed in the CS/CMC matrix uniformly. Finally, the mixture was poured on Teflon Petri dish and naturally air dried to a constant mass. Then the dried membrane was immersed into 5 wt% NaOH aqueous solution to remove the silica gel and the remaining acid. To improve the crosslinking degree of the blend membranes, 2.18 g epichlorohydrin was added into the beaker and the reaction was carried out for 3 h. After the crosslinking procedure, the porous membranes were washed extensively with deionized water until pH was neutral and dried in an oven at 60°C for use. For comparison, CS/CMC dense membranes were fabricated using the above procedures of CS/CMC amphoteric blend membranes except for the absence of the silica gel.

### 2.3. Characterization and Measurement

**2.3.1. Characterization.** Attenuated total internal reflectance Fourier-transform infrared (ATR-FTIR) spectroscopy of the membrane was conducted using a Nicolet 6700 spectrometer (Thermo Scientific, USA) of over a 650-4000  $\text{cm}^{-1}$  range at a resolution of 4  $\text{cm}^{-1}$ . The surface and cross-sectional micromorphology of the membranes were characterized by using scanning electron microscopy (FESEM, Hitachi, SU8010, Japan).

**2.3.2. Density Measurement of the Membrane.** The as-prepared membranes were washed several times with deionized water until the pH became neutral. After wiping up by filter paper and cut into a rectangular shape, the volume ( $V$ ) could be calculated by corresponding a length, width, and thickness. Afterwards, the square small pieces were dried to constant weight ( $m$ ). The membrane density ( $\rho$ ) was calculated by the following equations:

$$\rho = \frac{m}{V}. \quad (1)$$

**2.3.3. Pore Size Measurement of CS/CMC Blend Membranes.** The porosity of CS/CMC blend membranes was calculated by the following equation [23]:

$$\text{Porosity (\%)} = \left(1 - \frac{P_1}{P_2}\right) \times 100\%, \quad (2)$$

where  $P_1$  ( $\text{g/cm}^3$ ) and  $P_2$  ( $\text{g/cm}^3$ ) denote the microporous membrane and dense membrane density, respectively.

**2.3.4. Determination of Tobacco-Protein Adsorption-Desorption.** The adsorption of protein was as follows: the tobacco extract (0.5 g) was diluted with the buffer solution with varying pH values until the total volume of the solution was about 50 mL. Then 0.05 g CS/CMC blend membranes containing 20 wt% CMC were added into the above solution, followed by mechanical stirring at room temperature for 12 h. After that, the membranes were removed from the solution to measure protein content. After that, the above CS/CMC blend membrane-adsorbed proteins were added to the buffer solution with pH 8.36, 9.40, and 10.23 and then stirred at room temperature for 12 h. Afterwards, the membranes were removed from the solution to measure the protein content. The determination of supernatant protein was conducted by coomassie blue staining after centrifuging mixed solution of tobacco extract [24]. Adsorption capacity of the CS/CMC blend membranes from tobacco extract solution was studied at various pH values. The same method was carried out, when we changed adsorption time, CS/CMC content, initial protein concentration, and composition of CS/CMC blend membranes. Determination of tobacco protein in eluted solution is based on the reaction of coomassie brilliant blue G-250 with protein according to coomassie blue staining. The determination procedure is introduced as follows: the eluted solution (1 g) was added to deionized water (50 mL) in a flask and then stirred uniformly to pending solution. The aforementioned solution (0.05 mL) was moved to a test tube, and then sodium hydroxide of 0.15 mol/L was diluted to 1 mL solution. Afterwards, 5.0 mL coomassie brilliant blue G-250 was added into the above test tube and mixed on the vortex mixers. Finally, the as-prepared solution was measured at 595 nm with a Lambda 35 ultraviolet visible spectrophotometer (Cary-50, Varian Co., USA). The concentration of protein was calculated with the standard protein curve, which was calibrated by different concentrations of bovine serum albumin.

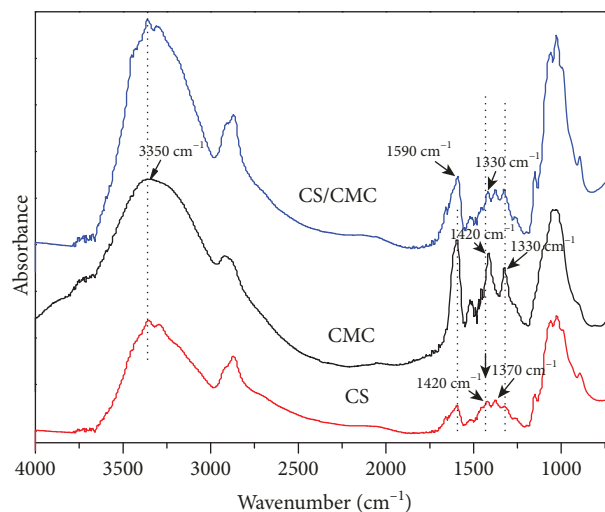


FIGURE 1: ATR-FTIR spectra of CS, CMC, and CS/CMC membranes.

The amount of adsorbed protein was calculated using the following expression.

$$\text{Adsorption capacity} = (C_0 - C_1) \times \frac{V}{W}, \quad (3)$$

where  $C_0$  ( $\text{mg/cm}^3$ ) and  $C_1$  ( $\text{mg/cm}^3$ ) are the initial and final concentrations, respectively, of the ovalbumin solution,  $V$  ( $\text{cm}^3$ ) is the volume of the ovalbumin solution, and  $W$  (mg) is the weight of the dry CS/CMC blend membranes. All the adsorption data were averages of at least five experiments.

### 3. Results and Discussion

**3.1. Characterization of CS/CMC Amphoteric Ion Exchange Membranes.** Figure 1 shows the structure of CS, CMC, and CS/CMC membranes. As presented in the spectrum of CS, the characteristic peak at  $3350 \text{ cm}^{-1}$  is assigned to the stretching vibration of -OH, which is not only shifted to a lower wavenumber but also become wide because of the existence of hydrogen bonding between the hydroxyl groups of molecular chains [25]. The characteristic peak at  $2920 \text{ cm}^{-1}$  is attributed to the C-H stretching vibration. Moreover, a peak at  $1590 \text{ cm}^{-1}$  (related to the C=O stretching vibration of carboxymethyl) is shifted to a lower wavenumber as a result of the effect of the lone pair electrons on the adjacent oxygen atoms [26]. Simultaneously, the bands at  $1420 \text{ cm}^{-1}$  and  $1330 \text{ cm}^{-1}$  are ascribed to the in-plane bending of -OH (on the different site of the backbones). A broad adsorption band at  $1050 \text{ cm}^{-1}$  is ascribed to the overlapping of adsorption bands of different C-O stretching vibrations. Compared to CMC, CS exhibits two bands at  $3350$  and  $3290 \text{ cm}^{-1}$  corresponding to -OH and -NH stretching vibrations, respectively. Furthermore, the characteristic peak at  $1590 \text{ cm}^{-1}$  is weaker than that of CMC due to the high degree of deacetylation of CS. The characteristic peaks at  $1420$  and

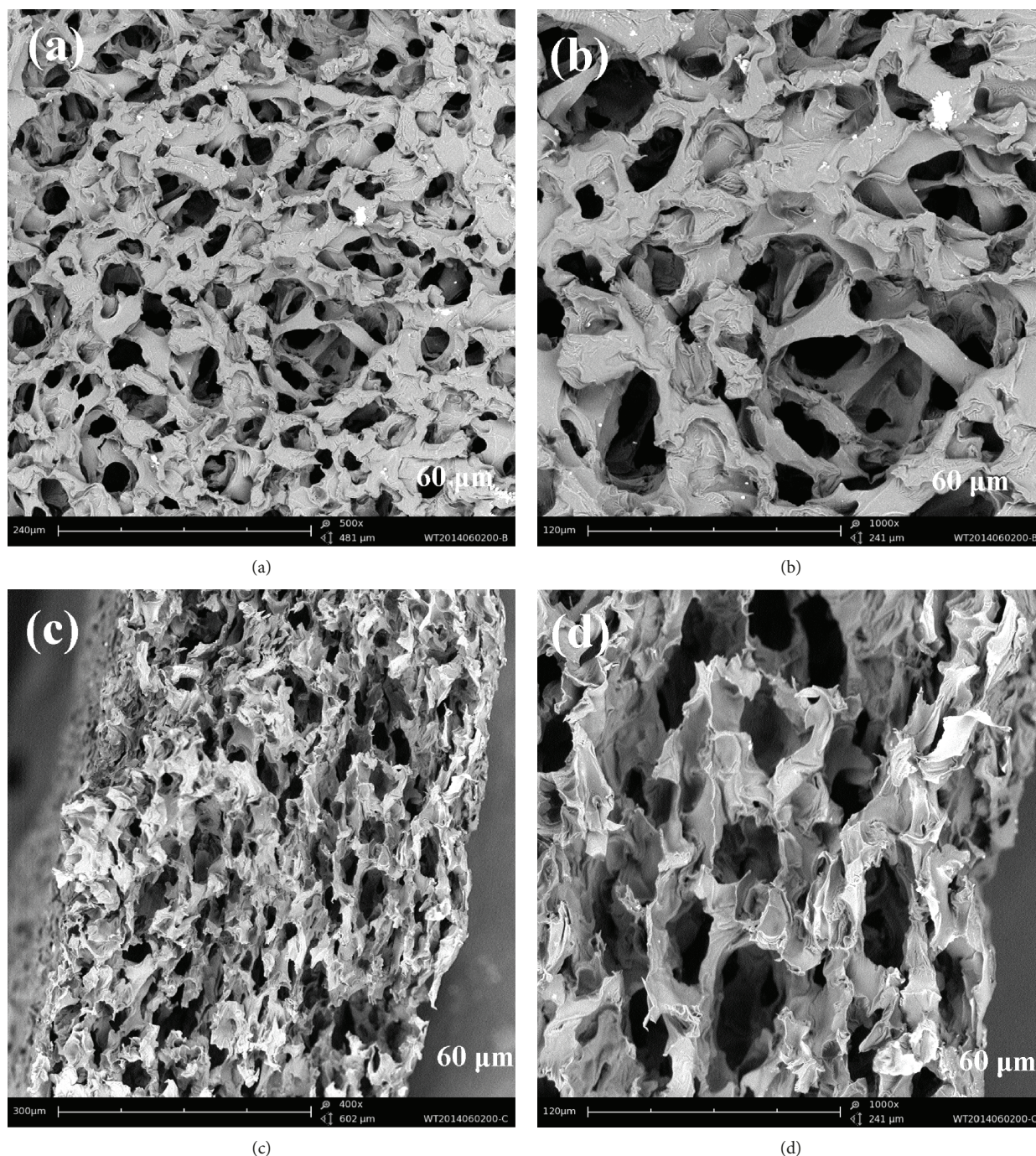


FIGURE 2: SEM images of CS/CMC blend membranes with the CMC content of 20 wt%: (a) surface, 500x; (b) surface, 1000x; (c) cross-section, 500x; (d) cross-section, 1000x.

$1370\text{ cm}^{-1}$  are assigned to the out-of-plane bending of  $-\text{OH}$ , which may be overlapped by the adsorption bands of  $-\text{CH}$  in-plane bending [27]. The peak corresponding to overlapping of different adsorption bands of  $\text{C}-\text{O}$  stretching vibration also can be observed at  $1050\text{ cm}^{-1}$  in the FTIR spectrum of CS [28]. Compared to CS, the characteristic peak at  $1590\text{ cm}^{-1}$  is strong in the spectra of the CS/CMC membrane. At the same time, the new peak at  $1330\text{ cm}^{-1}$  originating from the in-plane bending of  $-\text{OH}$  is notable in the spectrum, which is in good agreement with the typical characteristic

peak of CMC [29], indicating the successful preparation of the CS/CMC blend membranes.

SEM images were obtained to further explore the surface and cross-sectional morphology of the membranes. As shown in Figures 2(a) and 2(b), the pore with a three-dimensional opening structure was uniformly distributed in the surface of the membrane, which had an average pore diameter ranging from 30 to 50 μm. The pores were connected with each other, which could be good for the passage of the solution, and increased the contact area of the solution

TABLE 1: Physical characteristics of the macroporous CS/CMC blend membranes.

Sample	CS : CMC = 80 : 20 (200-300)		CS : CMC = 60 : 40 (200-300)		100% CS (200-300)	
	Dense	Porous	Dense	Porous	Dense	Porous
Disposition	Dense	Porous	Dense	Porous	Dense	Porous
Density ( $\text{g}/\text{cm}^3$ )	0.3996	0.2221	0.4529	0.2684	0.4237	0.1949
Pore size ( $\mu\text{m}$ )	—	30-50	—	20-40	—	30-50
Porosity (%)	—	54.53	—	40.74	—	54.00

and the membrane pore wall. The cross-sections of the blend membranes were shown in Figures 2(c) and 2(d), the pore of the CS/CMC blend membranes was connected with each other, which was distributed uniformly in the cross-section of the blend membranes with the thickness of 300-350  $\mu\text{m}$ , and pore structure had strong stereoscopic effect. Furthermore, it is observed that the pore structures did not collapse. CS/CMC blend membranes did not show phase separation, which exhibited good miscibility due to the similarity in the molecular chain structures of CS and CMC. The density and porosity measurement were also conducted to investigate physical characteristics of CS/CMC blend membranes. It can be seen from Table 1 that the density of the pure CS membrane was  $0.4237 \text{ g}/\text{cm}^3$ , while the density of the CS dense membrane was only  $0.1949 \text{ g}/\text{cm}^3$ . The porosity of the pure CS membrane reached 54.00 wt%, which was ascribed to the good realized pore-forming effect of the membrane. The density and the porosity of CS/CMC blend membranes with the CMC content of 20 wt% were close to those of the pure CS membrane. However, the density of CS/CMC blend membranes increased with the increase of the CMC content, because the pores had collapsed. Therefore, the density reached  $0.2684 \text{ g}/\text{cm}^3$  and the porosity dropped to 40.74 wt%, when the CMC content was at 40 wt%.

### 3.2. Tobacco-Protein Adsorption Properties for Tobacco Protein

**3.2.1. Effect of the pH Value.** Figure 3 shows the effect of the pH value on the tobacco-protein adsorption properties of CS/CMC blend membranes. The medium pH was changed between pH 4.0 and 8.0. Adsorption capacity, which is defined as the amount of protein adsorbed per unit weight of the membrane, is used to evaluate the adsorption performance of the membrane. In the whole process of adsorption, CS/CMC blend membranes had considerable adsorption capacity at different pH values, indicating that the composition of tobacco protein was very complex and the isoelectric points were diverse. It also could be observed that the maximum adsorption capacity reached  $271.78 \text{ mg}/\text{g}$  at pH 6.15. These are ascribed to the electrostatic interaction between negatively charged tobacco protein and positively charged CS/CMC blend membranes was the strongest at around pH 6.15 and provided the highest adsorption capacity. The isoelectronic (pI) value of tobacco protein is 6.15. The pH value of buffer solution increased gradually. When the pH value exceeded 7, CMC in the ion exchange membrane dissolved gradually, while the protein adsorption capacity decreased due to the electrostatic repulsion between the

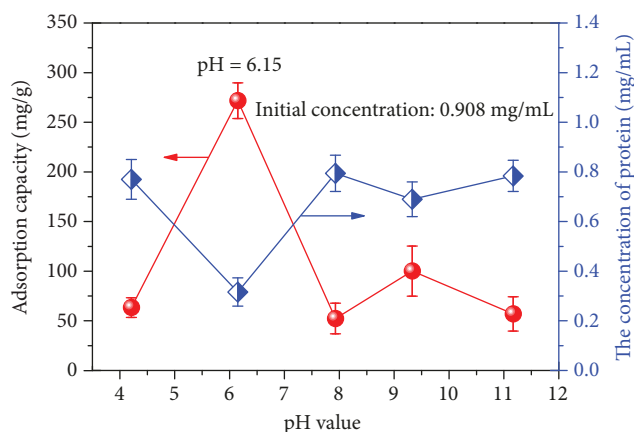


FIGURE 3: Effect of the pH value on the protein adsorption properties of the CS/CMC blend membranes.

negative charges of the blend membrane and acidic protein in tobacco. However, the adsorption capacity exhibited another peak at pH 9.33, which was attributed to a part of positively charged basic protein with high isoelectric point. As a result, the adsorption capacity increased. Furthermore, the adsorption capacity decreased gradually at pH 11.17, because the pH value exceeded the isoelectric point of the adsorbed protein. The electrostatic repulsion resulted in the decline of adsorption capacity, when the protein was negatively charged. The concentration of protein was also shown in Figure 3. In these cases, the changes of the concentration have opposite tendency with the changes of the adsorption capacity.

**3.2.2. Effect of Adsorption Time.** Figure 4 shows the effect of adsorption time on the protein adsorption properties of the CS/CMC blend membranes with the CMC content of 20 wt%. As shown in Figure 4, the concentration of protein gradually decreased with the adsorption time and leveled off up to 8 h. It was found that the adsorption capacity of the blend membranes increased with the increase of adsorption time. And then the adsorption capacity reached a constant value of  $252.50 \text{ mg}/\text{g}$  starting from the 9th hour. The adsorption of tobacco protein reached an equilibrium after adsorbing for 8 h. This is attributed to adsorptive saturation of CS/CMC blend membranes for the protein.

**3.2.3. Effect of the CS/CMC Content.** In the adsorption process, the CS/CMC content is a key parameter that affects the adsorption capacity. A certain amount of tobacco extract (0.5 g tobacco extracts was diluted to the protein

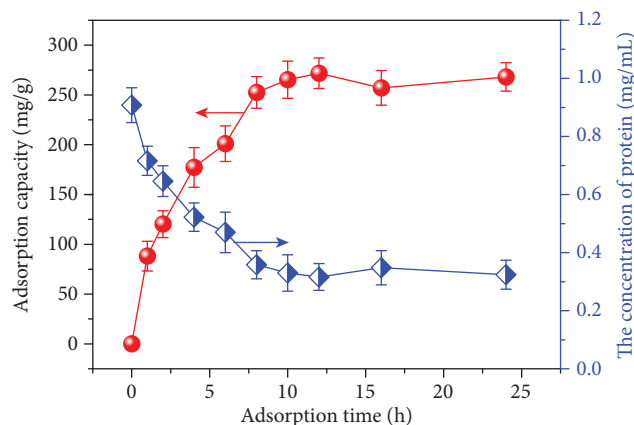


FIGURE 4: Effect of adsorption time on the protein adsorption of the CS/CMC blend membranes.

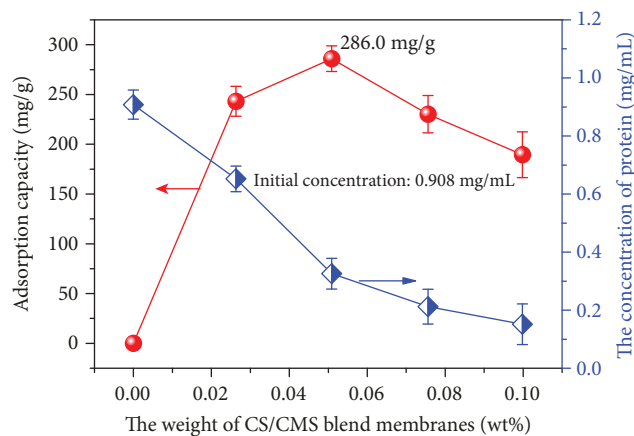


FIGURE 5: Effect of the CS/CMC blend membrane content on the protein adsorption.

concentration of 0.908 mg/mL) was tested to investigate the protein adsorption capacity using different CS/CMC contents. Figure 5 shows the effect of the CS/CMC blend membrane content on the protein adsorption properties. As shown in Figure 5, at the initial stage, the adsorption capacity of the membrane increased and then decreased with the increase of the CS/CMC content. The adsorption capacity of CS/CMC blend membranes was 243.16 mg/g, when the CS/CMC content reached 0.0236 g. At the meantime, the concentration of protein was also very high (up to 0.652 mg/mL), which may have an adverse effect on the quality of the tobacco extracts. When the CS/CMC content reached 0.051 g, the maximum adsorption capacity and the concentration of protein were 286 mg/g and 0.326 mg/mL, respectively. Though the concentration of protein decreased gradually, the adsorption capacity of the membrane dropped quickly, resulting in the decline of the application efficiency. In summary, the CS/CMC content was determined not only by the adsorption capacity but also by the concentration of the protein dissolved in the tobacco extract solution after adsorption. Therefore, the optimal CS/CMC content was approximately 0.05 g (the mass ratio of dry membrane to tobacco extract was 1 : 10).

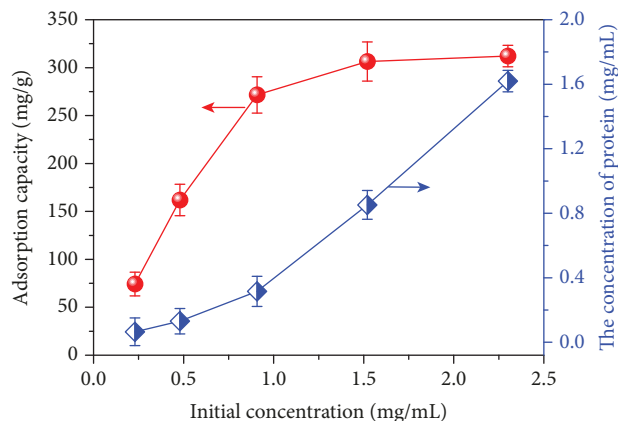


FIGURE 6: Effect of the initial protein concentration on the protein adsorption properties of the CS/CMC blend membranes.

**3.2.4. Effect of the Initial Protein Concentration.** The protein adsorption was a complex process, which was also affected by the initial protein concentration. The low concentration not only influenced the protein adsorption capacity but also increased the cost of the solution concentration. However, the high concentration was beneficial to the low adsorption capacity of the blend membranes due to high viscosity of solution. To study the relationship between the initial protein concentration and the protein adsorption capacity of the CS/CMC blend membranes, the tobacco-protein adsorption capacity of different initial protein concentrations with the same volume was tested. Figure 6 shows the effect of the initial protein concentration on the protein adsorption of the CS/CMC blend membranes. As shown in Figure 6, the adsorption capacity of the CS/CMC membranes increased with the initial protein concentration and then leveled off at 1.52 mg/mL with a saturated adsorption of 244.23 mg/g. After that, the adsorption capacity value remained constant with the increase of the protein concentration. This could be explained by saturation of interacting groups of CS/CMC blend membranes with the adsorbed protein molecules, as a result of which maximum adsorption capacity is achieved. Therefore, the optimal initial protein concentration was around 1.52 mg/mL.

**3.2.5. Effect of the Composition of CS/CMC Blend Membranes.** To determine the effect of the CS/CMC composition on the adsorption capacity, the adsorption experiments were performed with the initial protein concentration of 0.908 mg/mL at pH 6.15 as shown in Figure 7. As mentioned above, the blend membranes with amine groups were positively charged, while the protein was negatively charged at pH 6.15; in that time, a number of the amine groups acted as adsorption sites. However, the results were in contrary to those in Figure 7. The adsorption capacity gradually increased with the CMC content, and then reached a maximum value of 271.78 mg/g with the CMC content of 20 wt%. After that, the adsorption capacity dropped abruptly, when the CMC concentration exceeded 20 wt%, which was likely due to the fact that the high

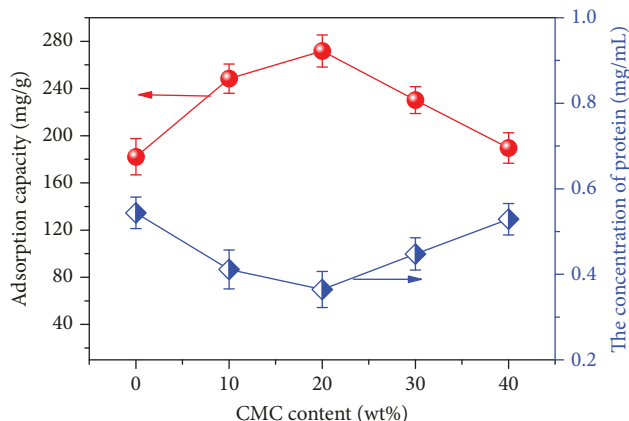


FIGURE 7: Effect of the CS/CMC composition on the protein adsorption properties of the CS/CMC blend membranes.

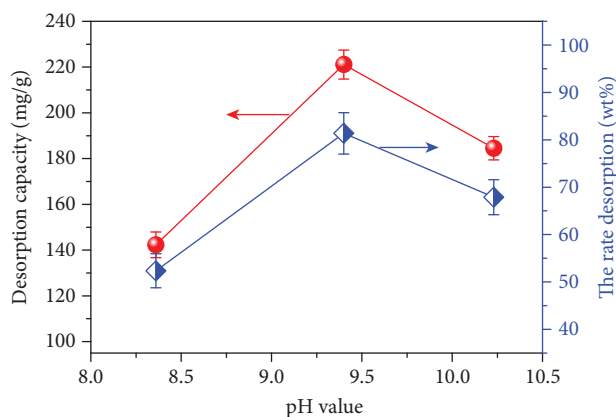


FIGURE 8: Effect of the pH value on the protein desorption properties of the CS/CMC blend membranes.

carboxymethyl group density on the surface of the membranes has caused large steric hindrance when the CMC content increased. As a result, the protein molecules were hindered from being close to the membranes and the adsorption capacity decreased. Similar results can be found in literature [30].

### 3.3. Protein Desorption of the CS/CMC Amphoteric Ion Exchange Membranes

**3.3.1. Effect of the pH Value on the Tobacco-Protein Desorption.** Figure 8 shows the effect of pH values on the tobacco protein desorption. The effective way to separate adsorbed proteins is to change the acidic environment of the elution liquid, which carried an opposite charge with that of the CS/CMC blend membranes. The desorption of the adsorbed protein from the CS/CMC blend membranes was performed in a buffer of the pH value of up to 7, which made protein elute from blend membranes with negative charge. When the pH value of the desorption solution increased, the adsorbed protein was found to be gradually desorbed from the membranes which was negatively charged in a desorption medium ( $\text{pH} > 7$ ). As shown in Figure 8, the

TABLE 2: Adsorption-desorption cycle stability of the CS/CMC blend membranes for tobacco protein.

	1	2	3
Adsorption capacity (mg/g)	$271.78 \pm 10$	$235.54 \pm 11$	$218.34 \pm 8$
Desorption capacity (mg/g)	$221.12 \pm 7$	$201.35 \pm 10$	$185.35 \pm 9$
Desorption efficiency (wt%)	$81.36 \pm 9$	$85.48 \pm 14$	$84.89 \pm 10$

CS/CMC membranes were negatively charged at pH 8.36. The tobacco protein was gradually desorbed from the membrane due to the electrostatic repulsions between the protein and the membrane. However, the efficiency of desorption is as low as 52.37%, which can be explained by the case that not all CMC carboxyl sites could be negatively charged at the low pH value. The efficiency of desorption increased to 81.36% dramatically, when the pH value increased to 9.36. The further increase of the pH value of eluted solution led to a sharp decrease in efficiency of desorption. This may be due to the strong basic strength of the buffer solution, resulting in the shrink of the membrane structure. Thus, the tobacco-protein adsorbed from the membrane cannot be desorbed easily. Therefore, the optimal pH value of eluted solution is 9.36.

**3.3.2. Tobacco Protein Adsorption-Desorption Cycle of the CS/CMC Membranes.** Table 2 shows the adsorption-desorption cycle stability of the CS/CMC blend membranes for tobacco protein. As shown in Table 2, the adsorption capacity decreased after adsorption-desorption cycles. The adsorption force of blend membranes for tobacco protein mainly originated from the electrostatic adsorption and the hydrogen bonding. Thus, complete desorption could not be achieved by adjusting the pH value. After the third adsorption-desorption cycle, the adsorption capacity of the membrane dropped from 271.78 mg/g to 218.34 mg/g, whose desorption efficiency exceeded 80%. This demonstrated that the membranes were of great reusability.

## 4. Conclusions

The amphoteric ion exchange membranes were prepared by blending CS with CMC using glutaraldehyde as a crosslinking agent and with silica particles as porogens. The membrane was applied to the adsorption of tobacco protein from the tobacco extract. This CS/CMC ion exchange membranes showed good adsorption-desorption properties for protein from tobacco extract. The adsorption capacity varied with the change of environmental pH, and the maximum of 271.78 mg/g was found at pH 6.15. The adsorption capacity of the blend membranes increased with the increase of adsorption time up to 8 h, and the adsorption capacity of CS/CMC blend membranes was 243.16 mg/g when the CS/CMC content reached 0.0236 g. The adsorption capacity of the CS/CMC membranes increased with the initial protein concentration of up to 1.52 mg/mL, and the adsorption capacity reached a maximum value of 271.78 mg/g with the CMC content of 20 wt%. The adsorbed tobacco protein could

be desorbed by more than 81.36 wt% through a change in the pH of the aqueous medium. The repeated adsorption-desorption process revealed that the macroporous CS/CMC blend membranes had good properties for the adsorption of the protein from tobacco extract.

### Data Availability

The data used to support the findings of this study are available from the corresponding author upon request.

### Conflicts of Interest

The authors declare that there are no conflicts of interest regarding the publication of this paper.

### Acknowledgments

This work was financially supported by the Science and Technology Project of Yunnan Province (no. 2017ZE027) and the Science and Technology Project of China Tobacco Yunnan Industrial Co. Ltd. (no. 2015CP02).

### References

- [1] P. Li, X. Zhu, S. Hong, Z. Tian, and J. Yang, "Ultrasound-assisted extraction followed by dispersive liquid-liquid microextraction before gas chromatography-mass spectrometry for the simultaneous determination of flavouring compounds in tobacco additives," *Analytical Methods*, vol. 4, no. 4, pp. 995–1000, 2012.
- [2] H. Bin, S. Wang, F. Xie, and H. Liu, "Application of high performance liquid chromatography-evaporative light scattering detection in determination of water-soluble sugars and sorbitol in tobacco flavourings and casings," *Chinese Journal of Chromatography*, vol. 30, no. 3, pp. 298–303, 2013.
- [3] L. L. Huang, H. M. Baker, C. Meernik, L. M. Ranney, A. Richardson, and A. O. Goldstein, "Impact of non-menthol flavours in tobacco products on perceptions and use among youth, young adults and adults: a systematic review," *Tobacco Control*, vol. 26, no. 6, pp. 709–719, 2017.
- [4] C. Liu, Y. DeGrandpre, A. Porter et al., "The use of a novel tobacco treatment process to reduce toxicant yields in cigarette smoke," *Food and Chemical Toxicology*, vol. 49, no. 9, pp. 1904–1917, 2011.
- [5] Y. Liu, A. Li, X. Feng, X. Sun, X. Zhu, and Z. Zhao, "Pharmacological investigation of the anti-inflammation and anti-oxidation activities of diallyl disulfide in a rat emphysema model induced by cigarette smoke extract," *Nutrients*, vol. 10, no. 1, p. 79, 2018.
- [6] M. Onishi, T. Kobayashi, C. N. D'Alessandro-Gabazza et al., "Mice overexpressing latent matrix metalloproteinase-2 develop lung emphysema after short-term exposure to cigarette smoke extract," *Biochemical and Biophysical Research Communications*, vol. 497, no. 1, pp. 332–338, 2018.
- [7] J. T. Bahr, D. P. Bourque, and H. J. Smith, "Solubility properties of fraction I proteins of maize, cotton, spinach, and tobacco," *Journal of Agricultural and Food Chemistry*, vol. 25, no. 4, pp. 783–789, 1977.
- [8] Z. Teng and Q. Wang, "Extraction, identification and characterization of the water-insoluble proteins from tobacco biomass," *Journal of the Science of Food and Agriculture*, vol. 92, no. 7, pp. 1368–1374, 2012.
- [9] D. Balasubramaniam, C. Wilkinson, K. Van Cott, and C. Zhang, "Tobacco protein separation by aqueous two-phase extraction," *Journal of Chromatography A*, vol. 989, no. 1, pp. 119–129, 2003.
- [10] H. B. Li and X. R. Xu, "Separation and determination of fluoride in plant samples," *Talanta*, vol. 48, no. 1, pp. 57–62, 1999.
- [11] K. D. Brunnemann, B. Prokopczyk, M. V. Djordjevic, and D. Hoffmann, "Formation and analysis of tobacco-specific N-nitrosamines," *Critical Reviews in Toxicology*, vol. 26, no. 2, pp. 121–137, 1996.
- [12] J. Brand and U. Kulozik, "Impact of the substrate viscosity, potentially interfering proteins and further sample characteristics on the ion exchange efficiency of tangential flow membrane adsorbers," *Food and Bioprocess Processing*, vol. 102, pp. 90–97, 2017.
- [13] M. Polino, A. Luísa Carvalho, L. Juknaitė et al., "Ion-exchange membranes for stable derivatization of protein crystals," *Crystal Growth & Design*, vol. 17, no. 9, pp. 4563–4572, 2017.
- [14] Z. Zhou, Y. Yang, J. Zhang et al., "Ion-exchange-membrane-based enzyme micro-reactor coupled online with liquid chromatography-mass spectrometry for protein analysis," *Analytical and Bioanalytical Chemistry*, vol. 403, no. 1, pp. 239–246, 2012.
- [15] T. Xu, "Ion exchange membranes: state of their development and perspective," *Journal of Membrane Science*, vol. 263, no. 1–2, pp. 1–29, 2005.
- [16] L. Zarybnicka, E. Stranska, J. Machotova, and G. Lencova, "Preparation of two-layer anion-exchange poly(ethersulfone) based membrane: effect of surface modification," *International Journal of Polymer Science*, vol. 2016, Article ID 8213694, 8 pages, 2016.
- [17] H. A. Ezzeldin, A. Apblett, and G. L. Foutch, "Synthesis and properties of anion exchangers derived from chloromethyl styrene codivinylbenzene and their use in water treatment," *International Journal of Polymer Science*, vol. 2010, Article ID 684051, 9 pages, 2010.
- [18] N. L. Burns, K. Holmberg, and C. Brink, "Influence of surface charge on protein adsorption at an amphoteric surface: effects of varying acid to base ratio," *Journal of Colloid and Interface Science*, vol. 178, no. 1, pp. 116–122, 1996.
- [19] T. Chakrabarty and V. K. Shahi, "Modified chitosan-based, pH-responsive membrane for protein separation," *RSC Advances*, vol. 4, no. 95, pp. 53245–53252, 2014.
- [20] X. Chen, J. Liu, Z. Feng, and Z. Shao, "Macroporous chitosan/carboxymethylcellulose blend membranes and their application for lysozyme adsorption," *Journal of Applied Polymer Science*, vol. 96, no. 4, pp. 1267–1274, 2005.
- [21] Z. Feng, Z. Shao, J. Yao, Y. Huang, and X. Chen, "Protein adsorption and separation with chitosan-based amphoteric membranes," *Polymer*, vol. 50, no. 5, pp. 1257–1263, 2009.
- [22] C. Zhang, R. Lillie, J. Cotter, and D. Vaughan, "Lysozyme purification from tobacco extract by polyelectrolyte precipitation," *Journal of Chromatography A*, vol. 1069, no. 1, pp. 107–112, 2005.
- [23] Y. C. Yang, C. C. Chen, C. S. Huang, C. T. Wang, and H. C. Ong, "Developments of metallic anodes with various compositions and surfaces for the microbial fuel cells," *International Journal of Hydrogen Energy*, vol. 42, no. 34, pp. 22235–22242, 2017.

- [24] Q. Q. Liang and Y. S. Li, "A rapid and accurate method for determining protein content in dairy products based on asynchronous-injection alternating merging zone flow-injection spectrophotometry," *Food Chemistry*, vol. 141, no. 3, pp. 2479–2485, 2013.
- [25] R. Dorati, S. Pisani, G. Maffei et al., "Study on hydrophilicity and degradability of chitosan/poly(lactide-co-caprolactone) nanofiber blend electrospun membrane," *Carbohydrate Polymers*, vol. 199, pp. 150–160, 2018.
- [26] K. H. Bodek, K. M. Nowak, M. Kozakiewicz, A. Bodek, and M. Michalska, "Evaluation of microcrystalline chitosan and fibrin membranes as platelet-derived growth factor-BB carriers with amoxicillin," *International Journal of Polymer Science*, vol. 2015, Article ID 386251, 13 pages, 2015.
- [27] Z. Xu, G. Liu, H. Ye, W. Jin, and Z. Cui, "Two-dimensional MXene incorporated chitosan mixed-matrix membranes for efficient solvent dehydration," *Journal of Membrane Science*, vol. 563, pp. 625–632, 2018.
- [28] X. Li, G. Chao, L. Wang et al., "Preparation and BSA adsorption behavior of chitosan-arginine based nanofiber membranes," *Fibers and Polymers*, vol. 19, no. 5, pp. 941–948, 2018.
- [29] S. I. Miremadi, N. Shafiabadi, S. A. Mousavi, and M. S. Amini-Fazl, "Gas separation properties of crosslinked and non-crosslinked carboxymethylcellulose (CMC) membranes," *Scientia Iranica*, vol. 20, no. 6, pp. 1921–1928, 2013.
- [30] S. Y. Suen, S. Y. Lin, and H. C. Chiu, "Effects of spacer arms on cibacron blue 3GA immobilization and lysozyme adsorption using regenerated cellulose membrane discs," *Industrial & Engineering Chemistry Research*, vol. 39, no. 2, pp. 478–487, 2000.



**Hindawi**  
Submit your manuscripts at  
[www.hindawi.com](http://www.hindawi.com)

